

Preparation and Thermal Characterization of Poly(ethylene oxide)/Griseofulvin Solid Dispersions for Biomedical Applications

Iwona Stachurek,¹ Krzysztof Pielichowski²

¹Faculty of Environmental Engineering, Cracow University of Technology, 31-155 Kraków, Poland

²Department of Chemistry and Technology of Polymers, Cracow University of Technology, 31-155 Kraków, Poland

Received 11 December 2007; accepted 23 July 2008

DOI 10.1002/app.29181

Published online 30 October 2008 in Wiley InterScience (www.interscience.wiley.com).

ABSTRACT: In this work, a series of poly(ethylene oxide)/griseofulvin (PEO/gris) solid dispersions has been prepared and characterized by PLM, FTIR, DSC, and MT-DSC. It has been found that the crystalline phase morphology depends strongly on the PEO molecular weight and, in the PEO/gris systems, griseofulvin molecules stay in amorphous phase of PEO, which enhances the solubility of a drug and increases its biological access. For PEO-drug systems containing 5, 10, and 15% gris, FTIR bands due to stretching vibrations of the O—H groups were found at 3436, 3436, and 3413 cm^{-1} , respectively, whereby for pure

PEO 3400, they were located at 3513 cm^{-1} —the observed shift proves the existence of hydrogen bonds between PEO and griseofulvin. The presence of griseofulvin caused lowering of the systems' melting temperature in the whole concentration range and, as evidenced by MT-DSC results, recrystallization of PEO in the PEO/griseofulvin systems during melting does occur. © 2008 Wiley Periodicals, Inc. *J Appl Polym Sci* 111: 1690–1696, 2009

Key words: poly(ethylene oxide); griseofulvin; solid dispersion; phase transitions; DSC

INTRODUCTION

Many potential drug candidates are characterized by a low oral bioavailability. Among the techniques used to increase aqueous solubility/dissolution rate, the formulation of solid dispersions of a drug in polymer matrix is one of the most useful ones. These can be defined as molecular mixtures of poorly water-soluble drugs in hydrophilic carriers, which present a drug release profile that is driven by the polymer properties.^{1,2} A critical issue in the processing of solid dispersions is to elucidate the microstructure of the resulting product.³ Morphological features such as the degree of crystallinity of both carrier and drug, and particle size of the latter, have a deep effect on the properties of the drug dissolution.^{4,5} The mechanisms for the enhancement of the dissolution rate of solid dispersions have been proposed by several investigators.^{6–9} Drugs molecularly dispersed in polymeric carriers may achieve the highest levels of particle size reduction and surface area enhancement, which result in improved dissolution rates. Furthermore, no energy is required to break up the crystal lattice of a drug during dissolu-

tion process, and drug solubility and wettability may be increased in the presence of hydrophilic carriers.^{8–10} The use of polymeric solid dispersions to increase the dissolution rate and the bioavailability of poorly water-soluble drugs is now well established.^{1,3,5,11–13} Solid dispersions represent a useful pharmaceutical technique for increasing the dissolution, absorption, and therapeutic efficacy of drugs in dosage forms. An important factor influencing the properties of such solid dispersions is the method of preparation and the type of the carrier used. The solid dispersion of one or more active ingredients in an inert carrier or matrix in the solid state can be prepared by the solvent, melting, or solvent-melting methods.^{14–16}

Among different polymeric carriers, poly(ethylene oxide) (PEO) is one of the most commonly used matrices.^{17,18} Numerous attempts to understand the physicochemical principle behind the improvement of the dissolution of drugs by solid dispersion formulation with poly(ethylene oxide) (which is a non-toxic, water soluble polymer) have been reported.¹⁹ Mechanisms suggested to be responsible for the improved aqueous solubility/dissolution properties of solid dispersions include reduction of the particle size of the incorporated drug, formation of complexes, formation of solid solutions, transformation of the crystalline drug to the amorphous state, reduction of aggregation and agglomeration,

Correspondence to: K. Pielichowski (kpielich@usk.pk.edu.pl).

TABLE I
Composition of PEO/Gris Systems

Sample	Composition (w/w)
PEO 3400/griseofulvin	95/5
	90/10
	85/15
PEO 10000/griseofulvin	95/5
	90/10
	85/15
PEO 20000/griseofulvin	95/5
	90/10
	85/15

improved wetting of the drug, and solubilization of the drug by the carrier at the diffusion layer. It is highly acceptable that often more than one of these phenomena determine the rate and extent of dissolution,^{20–22} and it is therefore of primary importance to determine the PEO crystalline phase behavior in the presence of a drug during the thermal treatment.

In our study, we have applied griseofulvin (gris) which is a water-insoluble, antifungal antibiotic that is quite stable at high temperature. Griseofulvin is used to treat dermatophyte infections of the skin, nails, or hair, with mild forms effectively handled topically.²³ Some literature reports revealed that solid dispersions have increased the dissolution rate and gastrointestinal absorption of griseofulvin.^{23–26}

EXPERIMENTAL

Materials

PEO 3400 and griseofulvin were obtained from Sigma-Aldrich (Steinheim, Germany). PEO 10,000 and PEO 20,000 were purchased from Polysciences (Warrington, USA).

Preparation

Solid dispersions containing 5, 10, and 15% gris were prepared by dissolving a weighed amounts of PEO and drug in methanol (Table I); the solvent was then evaporated. The solubility test was performed in different solvents (e.g., distilled water, methanol, ethanol, chloroform, acetone, or dimethylformamide). It was found that methanol was the most efficient solvent—it is in agreement with literature reports showing that methanol is commonly used as a solvent in the preparation of solid dispersions for biomedical applications.

Techniques

DSC analysis was performed on a Netzsch DSC 200 differential scanning calorimeter, calibrated with cyclohexanone, mercury, indium, and bismuth. Samples (about 5 mg) were placed in aluminum pans

and sealed. DSC measurements were carried out at heating/cooling rate of 10 K/min over the temperature range of -20 to 200°C under argon atmosphere. MT-DSC measurements were performed under argon atmosphere on a Mettler-Toledo DSC 822. The thermal behavior of solid dispersions was studied at the heating/cooling rate $\beta = 1$ K/min, period of modulation was $p = 45$ s, and amplitude of modulation $A_T = 0.5$ deg. Morphology was investigated by using a polarized light microscopy (PLM) produced by PZO Warszawa. Fourier transform-infrared spectra (FTIR) were obtained on a Bio-Rad FTS 165 apparatus with a resolution of 2 cm^{-1} at the range of $4000\text{--}600\text{ cm}^{-1}$. Samples were prepared as KBr discs. The KBr/sample ratio was 40/1 (200 mg of KBr per 5 mg of sample).

RESULTS AND DISCUSSION

First, morphology of PEO/gris was investigated by polarizing light microscopy. The results indicate that the obtained morphology depends on PEO molecular weight and crystallization behavior. It is recognized that the crystallization of a polymer from the melt is a two stage process. First, a nucleation process must occur, followed by crystal growth. Two types of nucleation occur as a result of random order fluctuations in supercooled phase, whereas heterogeneous nucleation is induced by other surfaces, for example, small particles acting as impurities. The latter crystallization type governs the solidification process of PEO systems with gris. If the drug remains as isolated particles, that is, not dissolved into the molten carrier, the drug particles can act as a nucleating agent. PEO 3400 showed that it is an appropriate griseofulvin carrier in which drug molecules are not exposed to crystallization and stay in amorphous state (Fig. 1).

Better solubility of substance and increase of biological access of medicine weakly dissolved in

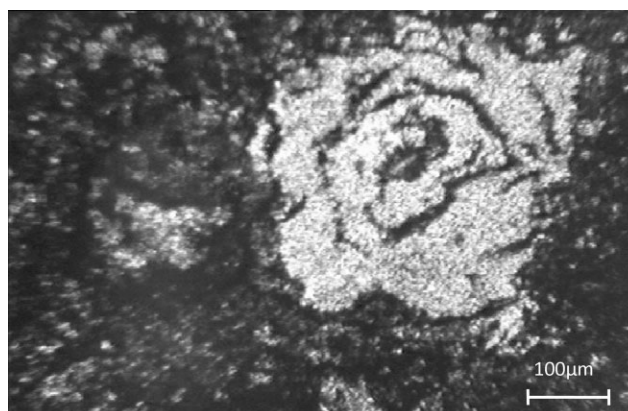


Figure 1 PLM microphotography of PEO 3400/griseofulvin system (90/10).

water is caused by larger participation of amorphous phase. Particles of gris did not undergo crystallization and their presence did not affect the crystallization course of polymer—it is of primary importance, because the presence of crystalline phase can cause changes in solubility profile and unfavorably influences the characteristics of drug. It has been recognized for a considerable period of time that pharmaceutical materials may also be prepared in an amorphous form where there is no long range order.^{27,28} Processes such as freeze and spray drying may lead to the generation of amorphous systems, while grinding or conventional drying may result in materials that are partially or wholly disordered. For instance, a ground mixture of griseofulvin and microcrystalline cellulose significantly improved both the dissolution rate and bioavailability of the drug compared to a micronised griseofulvin powder preparation.²⁹ This was ascribed to an increase in amorphous content of the drug as a result of the grinding process. Grinding of phenytoin with microcrystalline cellulose was also found to enhance drug dissolution rate, this again being attributed to the formation of an amorphous form of the drug.³⁰ Yang et al. applied melt granulation technique for gris-containing systems and found that a significant enhancement in the *in vitro* dissolution profiles of the granules was observed compared to the pure drug and drug excipient physical mixtures. The factorial design results indicated that higher drug loading and the presence of HPMC reduced the extent of dissolution of the drug, whereas, the presence of starch enhanced the dissolution rate. XRD data confirmed crystalline drug in formulation matrices. DSC results indicated monotectic mixtures of griseofulvin with PEG in the granulated formulations. Vigorous physical mixing of the binary systems apparently produced some amorphous drug (T_g during DSC). It was hypothesized that vigorous mechanical mixing also amorphosized some of the low-melting PEG

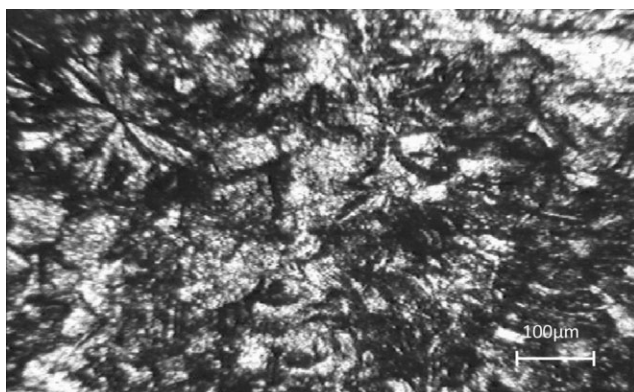


Figure 2 PLM microphotography of PEO 10,000/griseofulvin system (85/15).

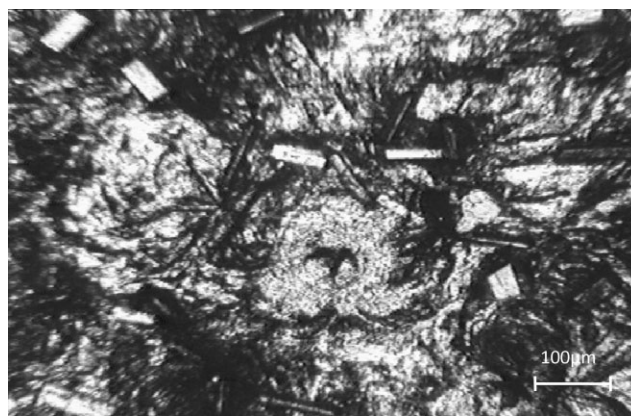


Figure 3 PLM microphotography of PEO 20,000/griseofulvin system (90/10).

material which combined with drug to produce lower melting monotectic drug/PEG mixtures. Some thermal curves suggest there may also be some higher melting crystalline drug not incorporated into monotectic drug/PEG mixtures.³¹ Generally, PEO crystallizes from the melt giving spherulites, which are spherical or disc-shaped formations with chain-folded lamellae radiating from a central point. Under polarized light, they can be recognized by the typical black Maltese cross.³² The size of crystals is dependent of crystallization temperature and cooling rate. Microphotographies of the solid dispersions of PEO 10,000 and PEO 20,000 with griseofulvin (Figs. 2 and 3) shown that polymer and drug are coparticipating in crystallization process.

To study possible interactions between PEO and gris, Fourier transform infrared spectroscopy was applied (Fig. 4).

Hydrogen bonding could be expected between the hydroxyl groups of PEO and oxygens present in the structure of griseofulvin. These interactions would

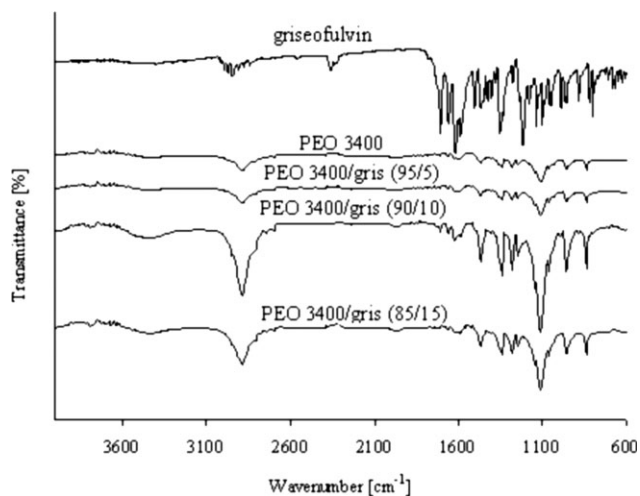


Figure 4 FTIR spectra of griseofulvin, PEO 3400 and PEO/grise systems.

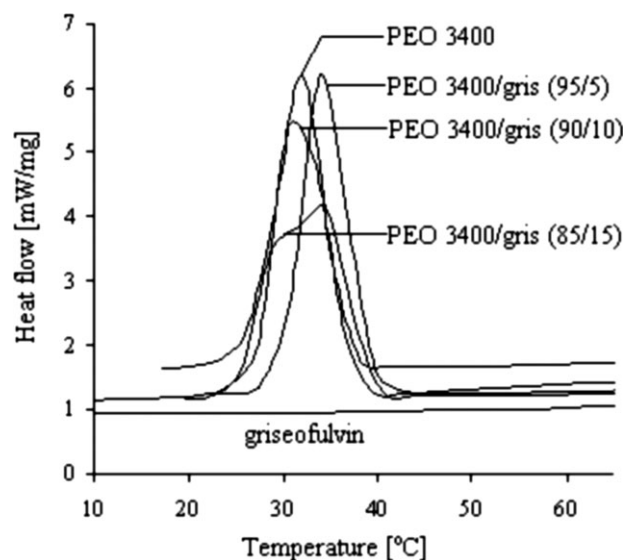


Figure 5 DSC profile of PEO 3400 and solid dispersion PEO 3400 with griseofulvin.

result in peak broadening and a bathochromic shift of the absorption bands of the interacting groups. FTIR spectrum of PEO 3400/griseofulvin solid dispersion does not differ substantially from the spectrum of pure PEO 3400. Similarly, spectra of PEO 10,000 and PEO 20,000/griseofulvin solid dispersions are similar to spectra of pure polymers. PEO, as a polyether, shows the C—O stretching vibration at 1112 cm^{-1} for PEO 3400, at 1110 cm^{-1} for PEO/griseofulvin (95/15), at 1112 cm^{-1} for PEO/griseofulvin (90/10) and PEO/griseofulvin (85/15). The spectrum of pure PEO 3400 displays one stretching vibration of the O—H group, which was found at 3513 cm^{-1} . For PEO-drug systems containing 5, 10, and 15% griseofulvin, these bands were found at 3436 , 3436 , and 3413 cm^{-1} , respectively. The observed shift proves the existence of hydrogen bonds between PEO and griseofulvin. At 2890 cm^{-1} weak, symmetric vibrations of the C—H in CH_2 groups were found, which was not found in the spectrum of pure griseofulvin. The spectra of solid dispersions and pure griseofulvin showed at $\sim 1600\text{ cm}^{-1}$ characteristic peaks for aromatic nucleus. Moreover, the spectrum of pure griseofulvin showed at $994\text{--}670\text{ cm}^{-1}$ deformation vibration of the $\text{C}_{\text{Ar}}\text{—H}$. Besides, two low-

intensity bands at 2942 and 2973 cm^{-1} were found—they originate from asymmetric, stretching C—H vibrations in CH_2 groups and were not detected for pure PEO 3400 and PEO/griseofulvin solid dispersions. Other characteristic vibrations were found for C=O at $\sim 1708\text{--}1618\text{ cm}^{-1}$ and these bands are of medium and high intensity. The bands of C—H vibrations in CH_2 groups showed medium or high intensity. They occur for PEO 3400 at 1470 cm^{-1} , PEO 3400/griseofulvin (95/5) at 1470 cm^{-1} , PEO 3400/griseofulvin (90/10) at 1469 cm^{-1} , and for PEO 3400/griseofulvin (85/15) at 1470 cm^{-1} . The peak at 1619 cm^{-1} (stretching vibrations of C=O and C=C) showed maximum intensity in griseofulvin. The bending vibrations of C—H bonds in CH_2 groups were found for PEO 3400 and solid dispersions at 1346 , 1148 , 961 , and 843 cm^{-1} . These bands displayed average or high intensity. For PEO 3400/griseofulvin systems the peak at 1061 cm^{-1} originates from deformation vibrations of C—Cl bond. The spectra of PEO 10,000, PEO 20,000 and solid dispersions containing 5, 10, and 15% of griseofulvin are similar to the spectra obtained for PEO 3400 and solid dispersions of this polymer with griseofulvin. It was found that hydrogen bonds between PEO 10,000 or PEO 20,000 and griseofulvin are also formed.

In the next stage, differential scanning calorimetry (DSC) was applied to study the phase transitions of the systems under investigation—results are presented in Figure 5 and Tables II and III.

Measurements were done for PEO 3400, griseofulvin, and for solid dispersions of PEO 3400 with griseofulvin because PLM analysis confirmed that griseofulvin in these systems stay in polymer amorphous phase. Analysis of crystallization course by DSC lead to conclusion that PEO 3400 includes integral folding chain (IF) crystals with extended chain crystals. PEO 10,000 and 20,000 crystallises forming lamellae with nonintegral folding chains (NIF) or with chains either fully extended (0) or folded once (1) or twice (2), depending on the crystallization conditions. The twice folded structure has a lower melting temperature with respect to that of the once folded. Similarly, the melting temperature of the once-folded chain crystal is lower than that of the extended chain crystals. IF crystals are produced by complete

TABLE II
Melting Parameters of PEO 3400, Griseofulvin, and PEO/Griseofulvin Systems

Samples	Melting				Heat of melting [J/g]
	$T_{\text{onset}} [^{\circ}\text{C}]$	$T_{\text{max1}} [^{\circ}\text{C}]$	$T_{\text{max2}} [^{\circ}\text{C}]$	$T_{\text{end}} [^{\circ}\text{C}]$	
PEO 3400	51,7	55,3	62,7	68,1	176,9
PEO3400/griseofulvin (95/5)	47,6	53,2	—	65,5	178,6
PEO3400/griseofulvin(90/10)	48,0	53,5	61,0	63,9	172,0
PEO3400/griseofulvin(85/15)	49,0	53,7	60,8	64,5	178,8
Griseofulvin	—	—	—	—	—

TABLE III
Freezing Parameters of PEO 3400, Gris, and PEO/Gris Systems

Samples	Freezing				Heat of crystallization [J/g]
	T_{onset} [°C]	T_{max1} [°C]	T_{max2} [°C]	T_{end} [°C]	
PEO 3400	36,5	32,0	–	27,4	173,4
PEO3400/gris(95/5)	36,6	31,5	–	28,4	172,2
PEO3400/gris(90/10)	39,0	34,3	29,7	25,7	166,6
PEO3400/gris(85/15)	39,1	34,2	–	30,0	175,8
Griseofulvin	–	–	–	–	–

crystallization of the polymer. NIF crystals are recognized as transitional states during crystallization and they are precursors of the crystal growth. Moreover, at low crystallization temperatures, NIF is thermodynamically the least stable crystalline state. IF crystals are resulted from transitions of nonintegral folding chains to integral folding chains through an isothermal thickening or thinning process.^{33,34} Which process occurs depends upon the thermodynamic driving force between the NIF and IF crystals and upon kinetic scheme. The majority of the NIF chain molecules conversion an isothermal thinning process to form IF ($n = 1$) crystals even though the field length of NIF crystal is thicker than that of the IF ($n = 1$) crystal. On the other hand, with increasing temperature, the fold length of NIF crystals increase continuously as does its thermodynamic stability. At a certain temperature, the thermodynamic stability of the NIF crystals is equal to thermodynamic stability of the IF ($n = 1$) crystals. Above that temperature, the nonintegral folding chain crystals still exist, but a transition from the NIF to IF ($n = 0$) crystals is identified through an isothermal thickening process. The relationship between the polymorphic behavior of PEO in a solid dispersion and the dissolution characteristics is of crucial importance in effective drug delivery systems.^{35,36} In PEO/gris systems, griseofulvin supplement caused lowering of the melting temperature and reduction of the degree of

crystallization. The DSC curves of the solid dispersions show one peak corresponding to the melting point of PEG 3400. As the griseofulvin content in the dispersion increases, the melting point of integral folding crystals and extended folding crystals becomes lower; for solid dispersion PEO 3400/gris (85/15) the melting point is 60.8°C. For solid dispersions PEO 3400/gris (95/5) and PEO 3400/gris (85/15) griseofulvin supplement caused higher heat of fusion of 178.6 and 278.8 J/g, respectively when compared to PEO (176.9 J/g). For solid dispersion, PEO 3400/gris (90/10) heat of fusion was 172.0 J/g. Comparison of the freezing point of solid dispersions and PEO 3400 reveals that in solid dispersions it is reduced. For PEO 3400 the freezing point is 32.3°C. The freezing point of PEO 3400/gris (95/5), PEO 3400/gris (90/10) and PEO 3400/gris (85/15) amounts to 31.5, 34.3, and 34.2°C, respectively. Some more information in comparison with traditional DSC can be obtained if modulated temperature DSC (MT-DSC) is used. Using this technique one can distinguish reversing and nonreversing components of the heat flow:

$$\frac{dQ}{dt} = C_p \frac{dT}{dt} + f(t, T) \quad (1)$$

where Q is the amount of heat absorbed of sample, C_p is the heat capacity, dT/dt is the heating rate, and $f(t, T)$ is a function of time and temperature

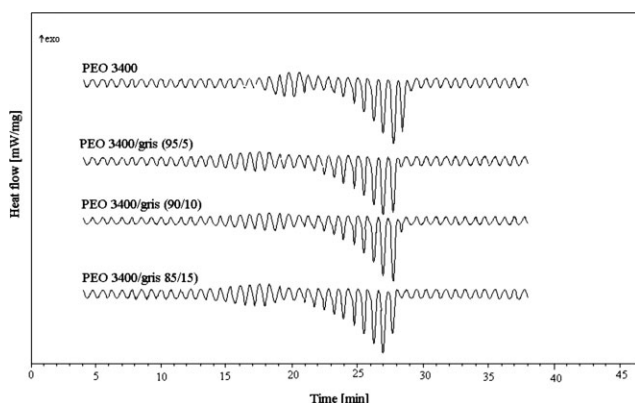


Figure 6 MT-DSC profiles of PEO and PEO/gris systems.

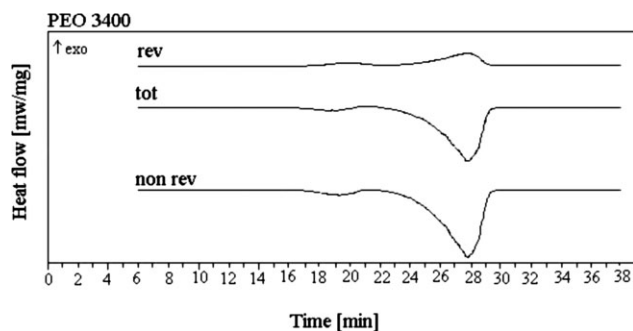


Figure 7 Total (tot), reversing (rev) and nonreversing (nonrev) MT-DSC signals of PEO 3400.

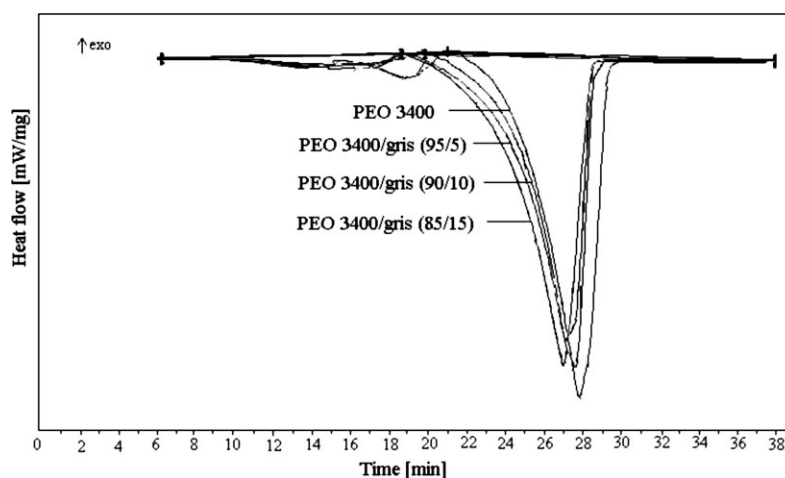


Figure 8 Nonreversing signals of PEO 3400 and PEO 3400/gris systems.

representing kinetic events. In MTDSC, the applied temperature program can be expressed as

$$T(t) = T_0 + \beta t + A \sin(\omega t) \quad (2)$$

where T_0 is the starting temperature, β is the underlying heating rate (equivalent to dT/dt), A is the amplitude of the temperature modulation and $\omega = 2\pi/p$ [1/s] is the modulation angular frequency. Equation 1 can be written as:

$$\frac{dQ}{dt} = C_p(\beta + A\omega \cos(\omega t)) + \bar{f}(t, T) + C \sin(\omega t) \quad (3)$$

where $\beta + A\omega \cos(\omega t)$ is the derivative modulated temperature, $\bar{f}(t, T)$ is the contribution to the total heat flow rate given by true irreversible events and C is the amplitude of the kinetic response to the modulation. The cyclic component of the heat flow signals depends on the value of β , ω , and C . In most kinetically controlled processes, C may be approximated to zero such that the response to the cyclic perturbation originates from the thermodynamic heat capacity contribution only and therefore eq. (3) can be written as:

$$\frac{dQ}{dt} = C_p(\beta + A\omega \cos(\omega t)) + \bar{f}(t, T) \quad (4)$$

The data may be averaged using a discrete Fourier transform algorithm and deconvoluted into reversing and nonreversing signals which relate to changes in C_p (thermodynamic events) and kinetic events, respectively. In conventional DSC, only the sum of the two components is determined and is called the total heat flow. Reversing heat flow in MT-DSC is a function of the sample's heat capacity and rate of temperature ($C_p dT/dt$) and the nonreversing is a function of temperature and time ($f(t, T)$). General recommendations for the choice of MT-DSC have been issued on the basis of experience that originates

from MT-DSC measurements of different polymeric systems.³⁷ Modulation period is usually between 40 and 100 s, underlying linear heating rate is about 1 to 5 K/min and the modulation amplitude is from ± 0.1 to ± 3 deg.³⁸ For the MT-DSC investigations of PEO/gris systems in the course of this work the following parameters were chosen: $p = 45$ s, $\beta = 1$ K/min and $A_T = 0.5$ deg.

Figure 6 presents a plot of the modulated heat flow for griseofulvin, PEO 3400 and solid dispersions of PEO with drug.

The total, reversing and nonreversing heat flows for the MTDSC experiment of pure PEO 3400 are shown in Figure 7.

One can observe endothermic melting (displayed in the nonreversing component of the heat flow) and exothermic recrystallization (displayed in the reversing signal). In comparison to the conventional DSC, separated signals shows the melting of the formed NIF and IF PEO crystals. For PEO 3400 and PEO 3400/gris solid dispersions two nonreversing endothermic signals were observed (Fig. 8).

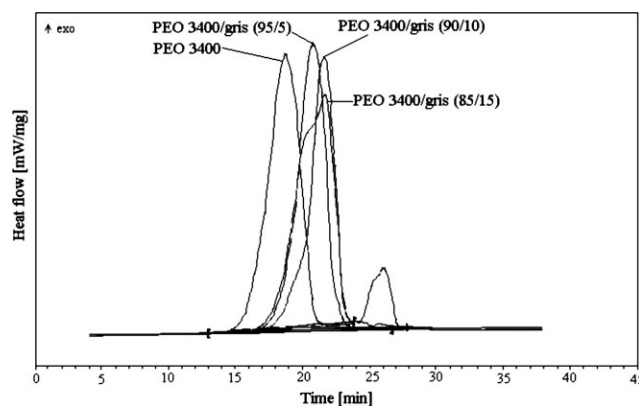


Figure 9 Reversing signal of PEO 3400 and PEO 3400/gris systems.

Exothermic reversing signal describes the crystallization process (Fig. 9).

The second peak on the reversing component of heat flow profile for the solid dispersion containing 10% gris may describe the recrystallization during heating. In the case of amorphous materials, there are two conflicting phenomena associated with the crystallization process. As the temperature is lower, the rate of nucleation may be expected to increase. However, the molecular mobility decreases as the temperature decreases, particularly below glass transition temperature (T_g), thereby slowing the molecular diffusion and reducing the rate of crystallization. Craig et al. showed that the maximum rate of crystallization will take place between melting point (T_m) and T_g . If a sample is stored below T_g , the risk of devitrification is considerably reduced due to the molecules having lower mobility with which to give in crystal growth.^{39,40}

CONCLUSIONS

The use of solid dispersions to increase the dissolution rate and the bioavailability of poorly water-soluble drugs is an important pharmaceutical issue. An important factor influencing the properties of such solid dispersions is the method of preparation and the type of the carrier used. On the other hand, the dissolution behavior of solid dispersions can be altered in storage due to changes in the physicochemical characteristics of the drug, the carrier, or both. The results of investigations show the suitability of PEO 3400 as the carrier for solid dispersions of griseofulvin because it stays in polymer amorphous phase. Generally, better solubility of medical substance and increase of biochemical access of drug weakly dissolved in water is caused by its preferential location in the amorphous phase. PEO 3400 includes integral folding chain (IF) crystals with extended chain crystals. Griseofulvin supplement caused melting temperature reduction in whole concentration range. Furthermore, FTIR data confirmed that hydrogen bonds between PEO and griseofulvin are formed.

References

1. Stachurek, I.; Pielichowski, K. *Arch Mater Sci* 2005, 26, 303.
2. Vasconcelos, T.; Sarmiento, B.; Costa, P. *Drug Discov Today* 2007, 12, 1068.
3. Martínez-Ohárriz, M. C.; Martín, C.; Goi, M. M.; Rodríguez-Espinosa, C.; Tros-Ilarduya, M. C.; Zornoza, A. *Eur J Pharm Sci* 1999, 8, 127.
4. Ginés, J. M.; Arias, M. J.; Moyano, J. R.; Sánchez-Soto, P. J. *Int J Pharm* 1996, 143, 247.
5. Verheyen, S.; Bleton, N.; Kinget, R.; Van den Mooter, G. *Int J Pharm* 2002, 249, 45.
6. Lloyd G. R.; Craig D. Q. M.; Smith A. *Eur J Pharm Biopharm* 1999, 48, 59.
7. Seo, A.; Holm, P.; Kristensen, H. G.; Schaefer, T. *Int J Pharm* 2003, 259, 161.
8. Craig, D. Q. M. *Int J Pharm* 2002, 231, 131.
9. Kim, E. J.; Chun, M. K.; Jang, J. S.; Lee, I. H.; Lee, K. R.; Choi, H. K. *Eur J Pharm Biopharm* 2006, 64, 200.
10. Taylor, L. S.; Zograf, G. *Pharm Res* 1997, 14, 1691.
11. Özkan, Y.; Doğanay, N.; Dikmen, N.; Isimer, A.; *Il Farmaco* 2000, 55, 4333.
12. Shakhshneider, T. P.; Vasilchenko, M. A.; Politov, A. A.; Boldyrev, V. V. *Int J Pharm* 1996, 130, 25.
13. Van den Mooter, G.; Augustijns, P.; Bleton, N.; Kinget, R. *Int J Pharm* 1998, 164, 67.
14. Stavchansky, S.; Gowan, W. *J Pharm Sci* 1984, 73, 733.
15. Alonso, M. J.; Maincent, P.; Garcie-Arias, T.; Vila-Jato, J. L. *Int J Pharm* 1988, 42, 27.
16. Tantishaiyakul, V.; Kaewnopparat, N.; Ingkatawornwong. *Int J Pharm* 1999, 181, 143.
17. Martínez-Ohárriz, M. C.; Martín, C.; Go, M. M.; Rodríguez-Espinosa, C.; Tros-Ilarduya, M. C.; Zornoza, A. *Eur J Pharm Sci* 1999, 8, 127.
18. Zalipsky, S. *Adv Drug Deliv Rev* 1995, 16, 157.
19. Bailey, F. E., Jr.; Koleske, J. V. *Poly(ethylene oxide)*; Academic Press: New York, 1976.
20. Calceti, P.; Salmaso, S.; Walker, G.; Bernkop-Schnürch, A. *Eur J Pharm Sci* 2004, 22, 315.
21. Greenwald, R. B. *J Control Release* 2001, 74, 159.
22. Finkelstein, E.; Amichai, B.; Grunwald, M. H. *Int J Antimicrob Agents* 1996, 6, 189.
23. Chiou, W. L.; Riegelman, S. *J Pharm Sci* 1969, 58, 1505.
24. Lo, W. Y.; Law, S. L. *Drug Dev Ind Pharm* 1996, 22, 231.
25. Saito, M.; Ugajin, T.; Nozawa, Y.; Sadzuka, Y.; Miyagishima, A.; Sonobe, T. *Int J Pharm* 2002, 249, 71.
26. Flego, C.; Lovrecich, M.; Rubessa, F. *Drug Dev Ind Pharm* 1988, 14, 1185.
27. Craig, D. Q. M.; Johnson, F. A.; *Thermochim Acta* 1995, 248, 97.
28. Craig, D. Q. M.; Royall, P. G.; Kett, V. L.; Hopton, M. L. *Int J Pharm* 1999, 179, 179.
29. Yamamoto, K.; Nakano, M.; Arita, T.; Nakai, Y. *J Pharmacokinetic Biopharm* 1974, 2, 487.
30. Yamamoto, K.; Nakano, M.; Arita, T.; Takayama, Y.; Nakai, Y. *J Pharm Sci* 1976, 65, 1484.
31. Yang, D.; Kulkarni, R.; Behme, R. J.; Kotiyan, P. N. *Int J Pharm* 2007, 329, 72.
32. Cheng, S. Z. D.; Barley, J. S.; Giusti, P. A. *Polymer* 1990, 31, 845.
33. Buckley, C. P.; Kovacs, A. J. *Colloid Polym Sci* 1975, 58, 44.
34. Buckley, C. P.; Kovacs, A. J.; *Colloid Polym Sci* 1976, 254, 695.
35. Cheng, S. Z. D.; Zhang, A.; Barley, J. S.; Chen, J. *Macromolecules* 1991, 24, 3937.
36. Cheng, S. Z. D.; Chen, J.; Zhang, A.; Barley, J. S.; Habenschuss, A.; Zschack, P. R. *Polymer* 1992, 33, 1140.
37. Pielichowski, K.; Flejtuch, K. *Polimery (Warsaw)* 2002, 47, 784.
38. Verdonck, E.; Schaap, K.; Thomas, L. C. *Int J Pharm* 1999, 192, 3.
39. Stachurek, I.; Pielichowski, K. *Mod Polym Mater Env Appl* 2006, 2, 177.
40. Coleman, N. J.; Craig, D. Q. M. *Int J Pharm* 1996, 135, 13.